

Clinical and Biological Correlates of Neurotoxicity Associated with CAR T-cell Therapy in Patients with B-cell Acute Lymphoblastic Leukemia

Bianca D. Santomaso^{1,2}, Jae H. Park^{3,4,5,6}, Darin Salloum⁷, Isabelle Riviere^{6,8}, Jessica Flynn⁹, Elena Mead¹⁰, Elizabeth Halton^{5,11}, Xiuyan Wang^{6,8}, Brigitte Senechal^{6,8}, Terence Purdon⁵, Justin R. Cross¹², Hui Liu¹², Behroze Vachha¹³, Xi Chen¹, Lisa M. DeAngelis¹, Daniel Li¹⁴, Yvette Bernal⁵, Mithat Gonen⁹, Hans-Guido Wendel⁷, Michel Sadelain^{5,6}, and Renier J. Brentjens^{3,4,5,6}

ABSTRACT

CD19-specific chimeric antigen receptor (CAR) T-cell therapy is highly effective against relapsed or refractory acute lymphoblastic leukemia (ALL), but is hindered by neurotoxicity. In 53 adult patients with ALL, we found a significant association of severe neurotoxicity with high pretreatment disease burden, higher peak CAR T-cell expansion, and early and higher elevations of proinflammatory cytokines in blood. Patients with severe neurotoxicity had evidence of blood-cerebrospinal fluid (CSF) barrier disruption correlating with neurotoxicity grade without association with CSF white blood cell count or CAR T-cell quantity in CSF. Proinflammatory cytokines were enriched in CSF during severe neurotoxicity with disproportionately high levels of IL6, IL8, MCP1, and IP10, suggesting central nervous system-specific production. Seizures, seizure-like activity, myoclonus, and neuroimaging characteristics suggested excitatory neurotoxicity, and we found elevated levels of endogenous excitatory agonists in CSF during neurotoxicity.

SIGNIFICANCE: We detail the neurologic symptoms and blood, CSF, and neuroimaging correlates of neurotoxicity associated with CD19 CAR T cells and identify neurotoxicity risk factors. Our findings implicate cellular components other than T cells and suggest novel links between systemic inflammation and characteristic neurotoxicity symptoms. *Cancer Discov*; 8(8); 958–71. ©2018 AACR.

INTRODUCTION

Multiple clinical trials of CD19-specific chimeric antigen receptor (CAR)-modified autologous T cells have demonstrated high rates of clinical responses in B-cell hematologic malignancies (1–9), leading to the recent approval by the FDA of two different CARs in relapsed/refractory B-cell acute lymphoblastic leukemia (B-ALL) and diffuse large B-cell lymphoma. Obstacles facing broad application of this immunotherapy include the unique treatment-related toxicities of cytokine release syndrome (CRS) and neurotoxicity that can

occur in some patients. These toxicities have been observed across all studies of CD19 CAR constructs incorporating either CD28 or 4-1BB costimulatory signaling domains (3, 4, 7–9) but appear to be more common in adult patients with acute lymphoblastic leukemia (ALL), often requiring deescalating doses of CAR T cells and protocol modifications (10–12).

Most reports to date have considered CRS and neurotoxicity in aggregate for toxicity reporting, but it is increasingly appreciated that CRS and neurotoxicity may occur exclusive of one another and with distinct timing and response to intervention. Although clinical and biological factors associated with CRS have been reported in several studies and the anti-IL6 receptor (IL6R) monoclonal antibody tocilizumab is approved for the amelioration of CRS (13), comprehensive clinical descriptions and analyses of neurotoxicity biomarkers are scarce, and there is no consensus on which therapeutic interventions are most effective for preventing or reducing the severity or duration of neurologic symptoms.

In addition to more common neurotoxicity symptoms such as encephalopathy, aphasia, delirium, tremor, and seizures, rare cases of rapid-onset and lethal diffuse cerebral edema have occurred in several clinical trials (11, 14, 15). A recent report points to early systemic inflammation as a trigger for endothelial cell activation and dysfunction during neurotoxicity in these cases (11). Using a nonhuman primate model of CAR T-cell neurotoxicity, others reported an association between neurotoxicity and elevated cerebrospinal fluid (CSF) cytokines IL6, IL2, GM-CSF, and VEGF as well as both CAR and non-CAR T-cell accumulation in the CSF and brain parenchyma (16). Despite these observations, the precise pathobiology of the neurotoxicity remains obscure. Better understanding of the clinical features and biological correlates of CAR T cell-associated neurotoxicity in patients is needed to identify pharmacologically targetable pathways to mitigate toxicity.

¹Department of Neurology, Memorial Sloan Kettering Cancer Center, New York, New York. ²Parker Institute for Cancer Immunotherapy, San Francisco, California. ³Leukemia Service, Department of Medicine, Memorial Sloan Kettering Cancer Center, New York, New York. ⁴Department of Medicine, Joan and Sanford Weill Medical College of Cornell University, New York, New York. ⁵Center for Cellular Therapy, Memorial Sloan Kettering Cancer Center, New York, New York. ⁶Center for Cell Engineering, Memorial Sloan Kettering Cancer Center, New York, New York. ⁷Cancer Biology & Genetics Program, Memorial Sloan Kettering Cancer Center, New York, New York. ⁸Michael G. Harris Cell Therapy and Cell Engineering Facility, Memorial Sloan Kettering Cancer Center, New York, New York. ⁹Department of Epidemiology and Biostatistics, Memorial Sloan Kettering Cancer Center, New York, New York. ¹⁰Department of Anesthesiology and Critical Care Medicine, Memorial Sloan Kettering Cancer Center, New York, New York. ¹¹Department of Nursing, Memorial Sloan Kettering Cancer Center, New York, New York. ¹²Donald B. and Catherine C. Marron Cancer Metabolism Center, Memorial Sloan Kettering Cancer Center, New York, New York. ¹³Department of Radiology, Memorial Sloan Kettering Cancer Center, New York, New York. ¹⁴Juno Therapeutics, Seattle, Washington.

Note: Supplementary data for this article are available at Cancer Discovery Online (<http://cancerdiscovery.aacrjournals.org/>).

B.D. Santomasso, J.H. Park, and D. Salloum share first authorship of this article.

Corresponding Authors: Jae H. Park, Memorial Sloan Kettering Cancer Center, 1275 York Avenue, New York, New York 10065. E-mail: parkj6@mskcc.org; and Renier J. Brentjens, E-mail: brentjer@mskcc.org

doi: 10.1158/2159-8290.CD-17-1319

©2018 American Association for Cancer Research.

To this end, we performed a comprehensive analysis of neurotoxicity in a large cohort of adult patients with relapsed B-ALL treated with CD19-specific 19-28z CAR T cells in a phase I clinical trial at Memorial Sloan Kettering Cancer Center (MSKCC; NCT0144069). We provide a detailed description of neurologic symptoms, neuroimaging, and blood and CSF correlates of neurotoxicity associated with CD19 CAR T cells. We identify a significant association of severe neurotoxicity with high pretreatment disease burden, higher peak CAR T-cell expansion in blood, and early and higher elevations of proinflammatory cytokines. Furthermore, we report a correlation between neurotoxicity grade and CSF protein levels, indicating blood-CSF barrier disruption, and evidence of central nervous system (CNS)-specific production of IL6, IL8, MCP1, and IP10. Finally, based on neuroimaging and symptoms suggestive of excitotoxicity, we hypothesized that endogenous excitatory agonists are involved in CAR-associated neurotoxicity and demonstrate elevated levels of the *N*-methyl-D-aspartate (NMDA) receptor agonists quino- linic acid and glutamate in CSF during CAR-associated neuro- toxicity, uncovering a potential pathophysiologic link between the complex systemic immune activation, the CSF cytokine profile, and neurologic symptoms associated with CD19 CAR.

RESULTS

Description of Neurotoxicity

Of the 53 patients who received 19-28z CAR T-cell infusions in the study, no patient developed fatal neurotoxicity or diffuse cerebral edema. Within 28 days of CAR T-cell infusion, 33 of 53 patients (62.3%) developed neurotoxicity of any grade. Eleven of 53 patients (20.8%) developed mild neurologic symptoms (9 grade 1; 2 grade 2). Twenty-two patients (41.5%) developed severe (grade ≥ 3) neurotoxicity: 19 patients (35.8%) developed grade 3 and 3 patients (5.7%) developed grade 4 neurologic events. The median time from CAR T-cell infusion to onset of first neurologic symptom of any grade was 5 days (range, 2–11 days) and the median time to the first severe neurotoxicity was 9 days (range, 2–11 days; Fig. 1A).

Among the 11 patients who developed mild neurotoxicity, mild encephalopathy or delirium, tremor, and headache were the most commonly observed neurologic symptoms (Supplementary Table S1). Mild encephalopathy had the appearance of disorientation to time or place, or impaired attention or short-term memory with preserved alertness. Patients retained the ability to name objects, follow simple commands, and communicate their needs. Waxing/waning of symptoms was observed frequently with worsening of encephalopathy during febrile episodes. Mild neurotoxicity was present for a median of 10 days (range, 1–14 days).

Severe neurotoxicity often began as mild somnolence, disorientation, impaired attention, and difficulty naming before progressing to global aphasia, myoclonus, depressed level of consciousness, encephalopathy, and seizures (Supplementary Table S1). Expressive aphasia was the most characteristic feature of severe neurotoxicity, developing in 21 of 22 severely affected patients, and was the first neurologic symptom in 19 of 22 patients. The aphasia was characterized by difficulty expressing language including impaired naming, paraphasic errors, and verbal perseveration. Expressive aphasia evolved over several

hours to global aphasia with expressive and receptive difficulty (grade 3 aphasia) in 19 patients. Patients with global aphasia often appeared awake but were mute and unable to follow commands. Other neurologic symptoms and signs of severe neurotoxicity included myoclonus, apraxia, frontal release signs, increased tone, pain, memory loss, meningismus, leg weakness, focal weakness, dysarthria, and facial automatisms.

In some cases, sudden changes in speech and facial automatisms with expressive aphasia resembled stroke or complex partial seizure, respectively, although cranial MRI was universally negative for ischemic stroke and electroencephalogram (EEG) typically showed frontal or diffuse slowing rather than subclinical seizure activity. Aphasia was clearly distinguishable from impaired attention or disorientation by mini mental status testing that was conducted daily on patients. The median duration of neurotoxicity in patients who developed severe symptoms was 11 days (range, 2–92 days), the same median duration as mild neurotoxicity.

Sixteen of 22 patients (72%) with severe neurotoxicity developed seizures that were generalized tonic-clonic, four with clinically apparent focal onset. We considered any grade seizure to be severe neurotoxicity. EEGs were performed on 30 patients, including all 22 patients (100%) with severe neurotoxicity, 1 patient with grade 2 neurotoxicity, and 7 patients with grade 1 neurotoxicity. The most common EEG findings were frontal intermittent rhythmic delta activity (FIRDA) and diffuse or frontal slowing with or without triphasic waves generally 2 to 3 Hz. Nonconvulsive status epilepticus (NCSE) has been reported with CD19 CAR T-cell therapy (17), and we found EEG evidence of NCSE in 2 patients, both of whom also had a clinical seizure. Four patients who had clinical seizure events during EEG monitoring had electrographic seizure activity evident on EEG. Seizure prophylaxis was added over the course of this study, but did not prevent seizures in those who received it. Seizure developed in 14 patients despite levetiracetam prophylaxis, but all seizures resolved with standard seizure management with benzodiazepine treatment and antiepileptic agent titration.

Neurotoxicity Correlated to Presence and Severity of CRS

There was a significant correlation of neurotoxicity with the presence and severity of CRS. All 33 patients who developed neurotoxicity had at least grade 1 CRS with fever ($\geq 38^\circ\text{C}$) preceding the onset of neurologic symptoms (Fig. 1B). We found a strong correlation between severe neurotoxicity and severe CRS [OR, 52.5 (8.66–1027.2) $P < 0.001$] and between severe neurotoxicity and grade of CRS [OR, 5.36 (2.52–15.74) $P < 0.001$]. Despite this correlation, severe neurotoxicity occurred without severe CRS in 8 patients and after fever alone in 5 (Fig. 1B).

The onset of neurologic symptoms in relation to CRS was variable. The median time to first neurologic symptoms and severe neurotoxicity was 5 and 9 days, respectively. Overall, the median onset of severe neurotoxicity from the beginning of CRS was 8 days (range, 1–11 days; Fig. 1A). Neurotoxicity sometimes occurred after CRS had completely resolved. Therefore, neurotoxicity typically occurs after the start of CRS, and severe neurotoxicity can occur simultaneously with or without severe CRS, although it is always preceded by at least fever.

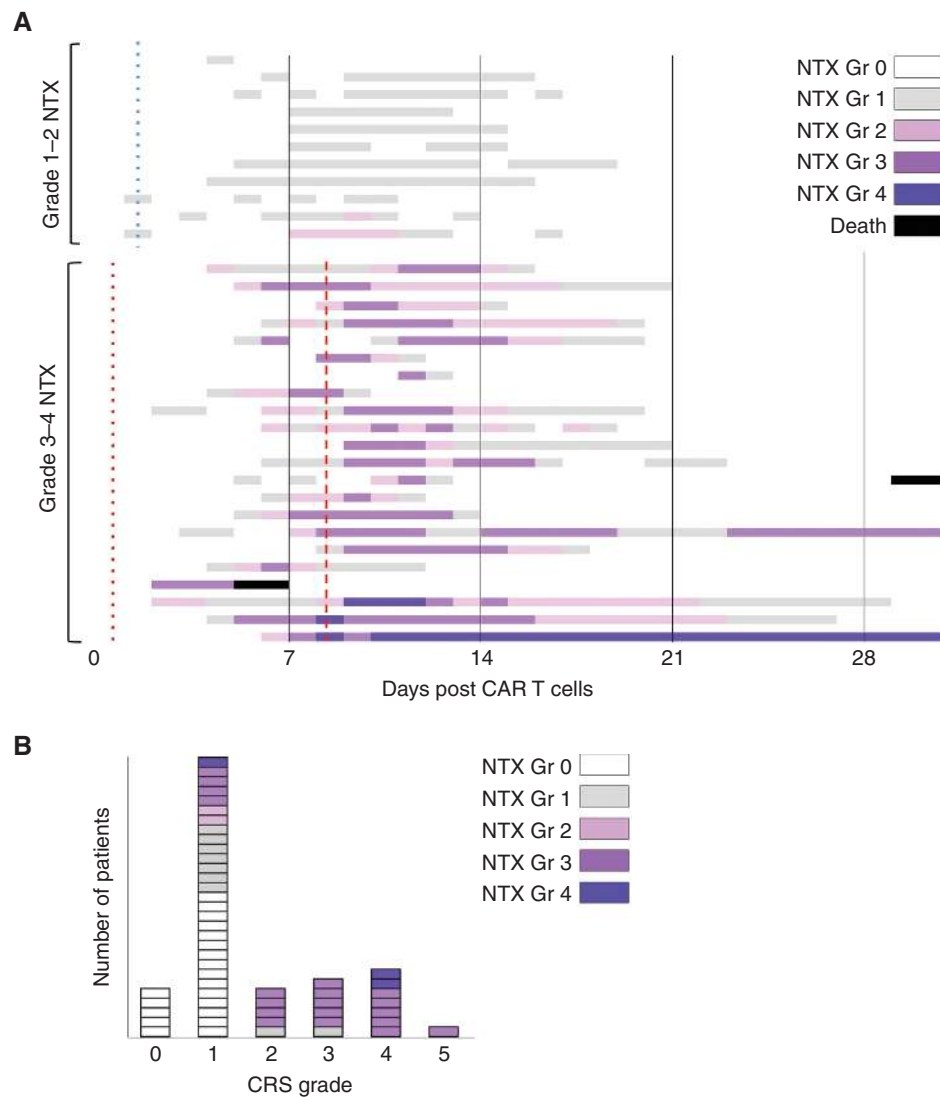


Figure 1. Timeline of neurotoxicity (NTX) and association with CRS after conditioning chemotherapy and 19-28z CAR T-cell infusion. **A**, Colors on the swimmer lane plot indicate the highest grade of any neurologic symptom recorded on each day for patients who developed grade ≥ 1 NTX through the first 30 days after CAR T infusion ($n = 33$; 11 grade 1-2 NTX, 22 grade 3-4 NTX). Two patients died within 30 days of CAR T-cell infusion (CRS, $n = 1$; sepsis, $n = 1$). Two patients had ongoing grade 3 or 4 NTX (sensorimotor neuropathy) at day 30 which improved to mild by days 39 and 96, respectively. Median time to first fever ($\geq 38^\circ\text{C}$) for patients with mild NTX (blue dotted line) and severe NTX (red dotted line) and median time to first severe (grade ≥ 3) NTX (red dashed line) are indicated. **B**, Number of patients with each grade of CRS and neurotoxicity.

Treatment of Neurotoxicity

The anti-IL6R monoclonal antibody tocilizumab, with or without corticosteroid, is often used to mitigate CRS and neurotoxicity. Six (18%) of 33 patients with neurotoxicity received tocilizumab alone; 14 (42%) received tocilizumab plus corticosteroid; 4 (12%) received corticosteroid alone; and 9 (27%) received neither tocilizumab nor corticosteroid (Supplementary Fig. S1). In the 16 patients with severe neurotoxicity who received tocilizumab, 9 (56.3%) had peak neurotoxicity after the first dose of tocilizumab, whereas 7 (43.7%) had peak neurotoxicity prior to or on the day of tocilizumab administration. Therefore, neurotoxicity did not respond to tocilizumab administration in most patients. The time from first tocilizumab and/or steroid dose to resolution of neurotoxicity (median, 9 days; range, 4-21 days)

was longer than the time to resolution of CRS (median, 1 day; range, 0-3 days; $P < 0.001$), confirming previous findings that neurotoxicity is less responsive than CRS to these treatment interventions. Serum cytokines, most notably IL6, but also IL8, IFN γ , G-CSF, and IL10 in some cases, peaked after tocilizumab administration (Supplementary Fig. S2).

Radiographic Findings of Neurotoxicity

MRI neuroimaging was obtained in 5 patients with grade 1 to 2 neurotoxicity and was normal in all. Fourteen of 22 patients who developed severe neurotoxicity had cranial MRI performed during acute symptoms. The MRI was normal in 9 patients, and 4 had a common pattern of T2/FLAIR hyperintensities involving the bilateral thalami and brainstem,

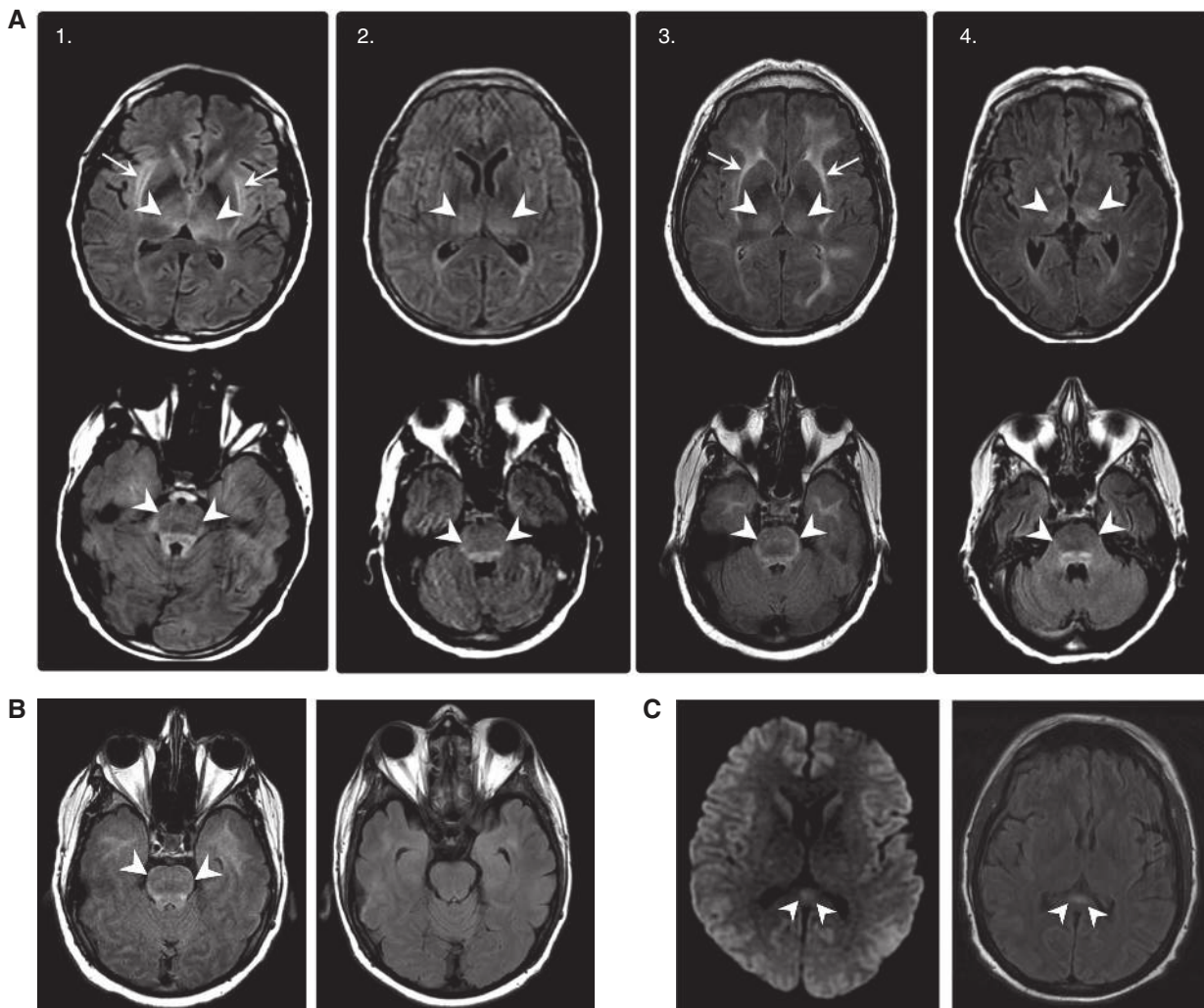


Figure 2. Brain MRI findings in patients with severe neurotoxicity after 19-28z CAR T-cell therapy. **A**, Axial FLAIR images demonstrate symmetric hyperintense signal abnormality in bilateral thalami (top, arrowheads) and the pons (bottom, arrowheads) in 4 patients (labeled 1–4) with acute neurotoxicity. Two patients (patients 1 and 3) demonstrate additional hyperintense signal abnormality in the extreme and external capsule (arrows). **B**, Brain MRI findings in a patient during (left) and after (right) resolution of acute symptoms of neurotoxicity. **C**, Axial DWI (left) and FLAIR (right) images in 2 patients with severe neurotoxicity demonstrating reversible lesions of the splenium of the corpus callosum (arrow) characterized by restricted diffusion (left, arrowhead) and FLAIR hyperintensity (right, arrowhead).

including the dorsal midbrain, dorsal pons, and medulla, extending to bilateral basal ganglia, extreme capsule, and brachium pontis in 2 patients (Fig. 2A). There was no diffusion restriction in these areas to suggest cytotoxic edema, and 2 patients who had follow-up neuroimaging after neurologic symptom resolution had reversal of the MRI changes (Fig. 2B). Another pattern observed was transient lesions of the splenium of the corpus callosum seen in 2 patients, characterized by restricted diffusion or T2/FLAIR hyperintensity (Fig. 2C). These lesions also resolved on subsequent imaging performed after neurologic symptom resolution.

Baseline Clinical and Posttreatment Biological Characteristics Associated with Neurotoxicity

In order to identify clinical and biological factors that are associated with severe neurotoxicity, we examined age, gender,

weight, body mass index, number of prior therapies, pretreatment disease burden, Philadelphia chromosome–positive (Ph+) ALL, CAR T-cell doses, prior hematopoietic stem cell transplant (HSCT) status, conditioning chemotherapy regimen, and infused CAR T-cell product characteristics. Using a Fisher exact test, we found a significant difference in pretreatment disease burden between patients who had severe versus mild neurotoxicity ($P = 0.002$; Table 1). Patients with high disease burden, defined as bone marrow blasts $\geq 5\%$ or radiographically evident extramedullary disease, were more likely to develop severe neurotoxicity. We did not find any association between $CD4^+/CD8^+$ ratio or phenotype (naïve, effector memory, effector) of the infused T-cell product and neurotoxicity (Supplementary Table S2). Univariate analysis showed a postinfusion higher peak CAR T-cell expansion in blood correlated to increased risk of severe neurotoxicity ($P < 0.001$; Fig. 3A).

Table 1. Patient characteristics associated with neurotoxicity

Neurotoxicity grade		Grades 0-2	Grades 3-4	Total	Univariate P
Overall, n (%)		31 (58)	22 (42)	53	
Age, n (%)	18-30	9 (29%)	5 (22.7%)	14 (26.4%)	0.04
	31-60	13 (41.9%)	16 (72.7%)	29 (54.7%)	
	>60	9 (29%)	1 (4.5%)	10 (18.9%)	
Gender, n (%)	Female	7 (22.6%)	6 (27.3%)	13 (24.5%)	0.753
	Male	24 (77.4%)	16 (72.7%)	40 (75.5%)	
Weight (kg)		78 (10.1-145.1)	80 (60.4-126)	78 (10.1-145.1)	0.752
BMI (kg/m ²)	<25	11 (35.5%)	8 (36.4%)	19 (35.8%)	1
	25-30	13 (41.9%)	9 (40.9%)	22 (41.5%)	
	>30	7 (22.6%)	5 (22.7%)	12 (22.6%)	
Lines of prior therapy	2	12 (38.7%)	9 (40.9%)	21 (39.6%)	1
	3	8 (25.8%)	5 (22.7%)	13 (24.5%)	
	≥4	11 (35.5%)	8 (36.4%)	19 (35.8%)	
Prior HSCT	No	20 (64.5%)	14 (63.6%)	34 (64.2%)	1
	Yes	11 (35.5%)	8 (36.4%)	19 (35.8%)	
Disease burden ^a	High	13 (41.9%)	19 (86.4%)	32 (60.4%)	0.002
	Low	18 (58.1%)	3 (13.6%)	21 (39.6%)	
Philadelphia chromosome	No	20 (64.5%)	18 (81.8%)	38 (71.7%)	0.223
	Yes	11 (35.5%)	4 (18.2%)	15 (28.3%)	
Conditioning chemotherapy	Flu/Cy ^b	5 (16.1%)	5 (22.7%)	10 (18.9%)	0.724
	Cy alone ^c	26 (83.9%)	17 (77.3%)	43 (81.1%)	
CAR T-cell dose (CAR T cells/kg)	1 × 10 ⁶	11 (35.5%)	10 (45.5%)	21 (39.6%)	0.752
	3 × 10 ⁶	19 (61.3%)	12 (54.5%)	31 (58.5%)	
	4 × 10 ⁵	1 (3.2%)	-	1 (1.9%)	
Cytokine release syndrome	None (grade 0)	14 (45.2%)	4 (18.2%)	18 (34%)	0.001
	Mild (grade 1-2)	16 (51.6%)	8 (36.4%)	24 (45.3%)	
	Severe (grade 3-5)	1 (3.2%)	10 (45.5%) ^d	11 (20.8%)	

Abbreviations: BMI, body mass index; HSCT, hematopoietic stem cell transplant; Flu, fludarabine; Cy, cyclophosphamide.

^aAll patients had disease burden assessed by bone marrow biopsy and/or radiographic studies prior to CAR T-cell infusion. High disease burden is defined as bone marrow blasts ≥5% or radiographically evident extramedullary disease. Low disease burden is defined as <5% bone marrow blasts.

^bFludarabine 25 mg/m²/d for 3-5 days and cyclophosphamide 1.5-3 g/m²/d for 1 day.

^cCyclophosphamide 1.5-3 g/m²/d for 1 day.

^dIncludes 1 patient who developed grade 5 CRS.

Severe Neurotoxicity Correlated with Systemic Inflammation

Patients who developed severe neurotoxicity had earlier fever onset and significantly higher day 3 and peak concentration of C-reactive protein (CRP) compared with those with mild neurotoxicity (Fig. 3B), suggestive of early inflammation. Ferritin concentration at day 3 but not peak ferritin level correlated with neurotoxicity severity (Fig. 3B). We observed a significant correlation between higher peak concentrations of several cytokines and severe neurotoxicity (Fig. 3C and D). Patients with severe neurotoxicity had higher levels of IL1 α , IL2, IL3, IL5, IL6, IL10, IL15, IP10, IFN γ , G-CSF, GM-CSF, and MCP1 by day 3 (Fig. 3C and D), suggesting that early rise and higher peak of these serum cytokines were associated with severe neurotoxicity. Low levels of EGF, made predomi-

nantly by platelets (18), also correlated with neurotoxicity (Fig. 3C and D). We found no significant difference in renal function in patients with severe neurotoxicity (Supplementary Fig. S3), and therefore serum cytokine elevations are not a result of altered clearance.

Because serum cytokines were significantly elevated by day 3 after CAR T-cell infusion (Fig. 3C and D), we examined them as predictive biomarkers of neurotoxicity. Using day 3 concentrations of IL10, IL15, and EGF, we separated patients into 3 groups with differing risks of severe neurotoxicity. Patients with low IL15 (<50 pg/mL) or high EGF (>120 pg/mL) have low risk of severe neurotoxicity [3/27; 11%; 95% confidence interval (CI), 2-29]. Patients with high IL15, low EGF, and low IL10 (<200 pg/mL) have an intermediate risk (9/15; 60%; 95% CI, 32-84), and patients with high IL15, low EGF,

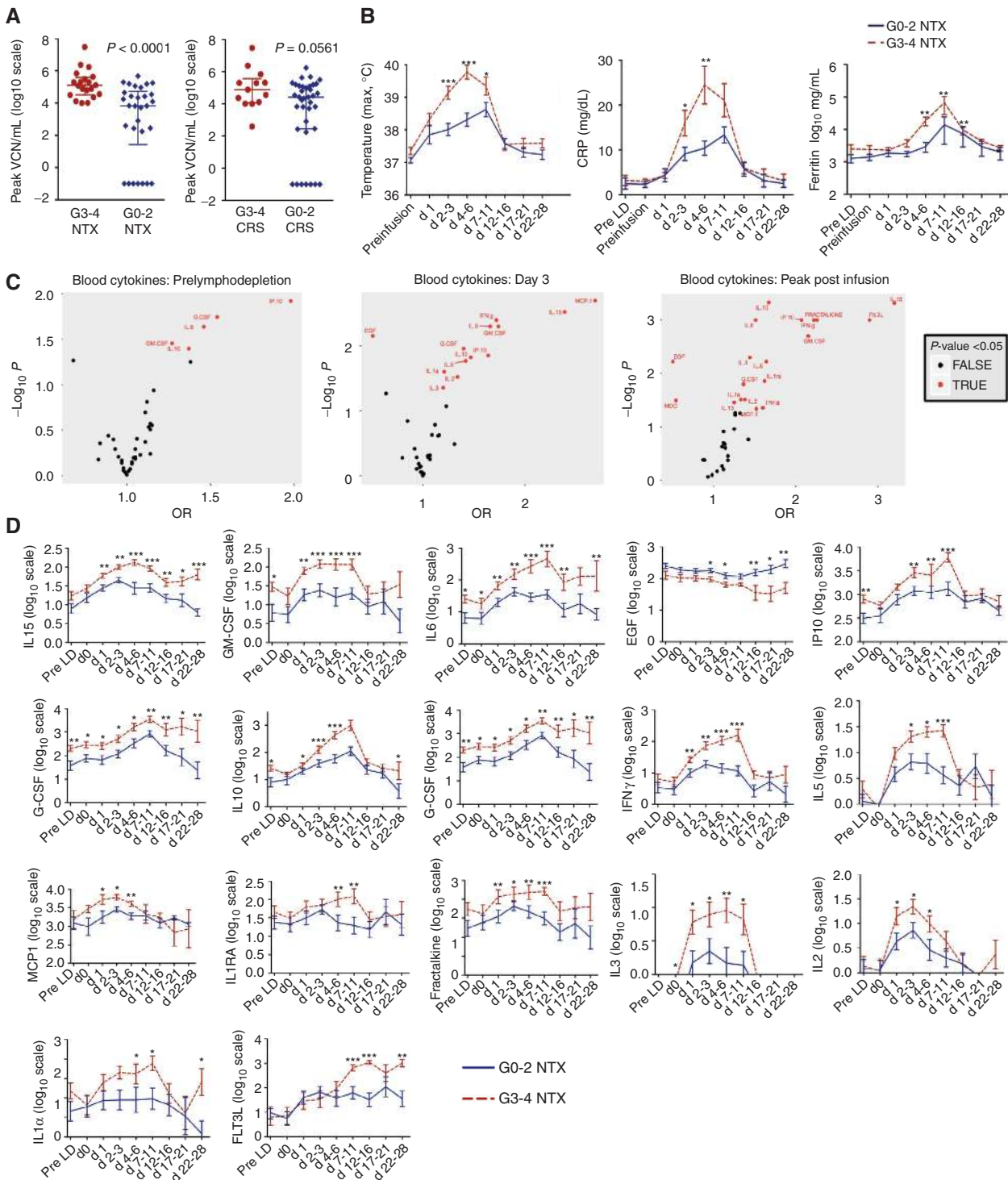


Figure 3. Systemic inflammation in patients with severe neurotoxicity (NTX). **A**, Severe NTX associated with higher peak CAR T expansion (vector copy number per mL) in blood. **B**, Maximum temperature, serum CRP, and ferritin are shown for patients at the indicated time windows after CAR T-cell infusion. **C**, Volcano plots visualizing the relative significance of serum cytokines associated with severe NTX by pre-lymphodepletion, day 3 after infusion, and peak after infusion during the first 28 days. Cytokines with $P < 0.05$ are indicated in red. **D**, Serum cytokine concentrations within indicated time windows comparing grade 0–2 versus grade 3–4 NTX for significant cytokines in **C**. All are maximum cytokine concentrations within the indicated time window except for EGF, which is minimum cytokine concentration. For **B** and **D**, Within each time window, the y-axis shows the mean \pm SEM of the values for all patients according to the NTX severity. P values were determined using the Kruskal–Wallis test. ***, $P < 0.001$; **, $0.001 < P < 0.01$; *, $0.01 < P < 0.05$. VCN, vector copy number; Pre-LD, prior to the start of lymphodepletion chemotherapy; d0, prior to CAR T-cell infusion; d, days after CAR T-cell infusion; G, grade.

Downloaded from <http://aacrjournals.org/cancerdiscovery/article-pdf/8/8/958/1840894/958.pdf> by guest on 27 August 2022

and high IL10 have high risk of severe neurotoxicity (10/10; 100%; 95% CI, 69–100).

Disseminated Intravascular Coagulation and Angiopoietins in Severe Neurotoxicity

Patients with severe neurotoxicity had a significantly higher incidence of laboratory markers of disseminated intravascular coagulation (DIC). Prothrombin time, activated partial thromboplastin time, and d-dimer were more elevated, and serum protein and albumin concentrations were decreased in patients with severe neurotoxicity, suggesting vascular leak following CAR T-cell infusion (Supplementary Fig. S3). More pronounced thrombocytopenia and fibrinogen nadir occurred 7 to 11 days following CAR T-cell infusion. Of the baseline laboratory parameters prior to conditioning chemotherapy, a lower baseline platelet count most significantly correlated with severe neurotoxicity. We found that low baseline platelet count ($\leq 50,000/\mu\text{L}$) and presence of fever ($\geq 38.0^\circ\text{C}$) on day 3 of CAR T-cell infusion identified 17 of 23 patients (73.9%) who proceeded to develop severe neurotoxicity.

The angiopoietin (ANG)–TIE2 axis, which regulates the balance between endothelial activation and quiescence, has recently been shown to be altered in patients with grade ≥ 4 neurotoxicity and CRS (11, 19). ANG1 is a protective factor that constitutively signals endothelial cells to maintain a quiescent state, whereas ANG2, a high-affinity TIE2 antagonist, remains sequestered in endothelial cell Weibel–Palade bodies until endothelial activation occurs (20). Because only 3 patients developed grade 4 neurotoxicity and no patient had grade 5 neurotoxicity in our study, we analyzed ANG1 and ANG2 levels in patients with grade 0 to 2 versus grade 3 to 4 neurotoxicity and CRS. In serum at 1 week after CAR T-cell infusion, we found significantly lower levels of the endothelial protective factor ANG1 and higher ANG2:ANG1 ratios in patients with severe neurotoxicity, and higher levels of ANG2 in patients with severe CRS compared with mild CRS (Supplementary Fig. S4). Although we did not find higher levels of ANG2 in patients with severe neurotoxicity, the ANG2:ANG1 ratios were significantly higher in patients with severe neurotoxicity, similar to the previous reported finding (11).

Blood–CSF Barrier Disruption, Proinflammatory Cytokines, and Excitotoxins in CSF from Patients with Severe Neurotoxicity

The CSF compartment is in close anatomic contact and communication with the brain interstitial fluid, and immunologic and biochemical changes related to CAR-associated neurotoxicity may be reflected in the CSF. We performed lumbar punctures in 20 patients with neurotoxicity (8 grade 1–2 and 12 grade 3–4) during the acute symptoms and in 1 patient without any neurotoxicity 14 days after CAR T-cell infusion. White blood cell (WBC) counts in the CSF were mildly increased, reflecting a pleocytosis relative to peripheral WBC counts. However, the CSF cell counts did not correlate with the neurotoxicity grade ($P = 0.492$; Fig. 4A and B). CSF samples were assessed by qPCR for CAR T cells. In 19 of 21 patients (95%), including patients with mild or no neurotoxicity, CAR T cells were detected in CSF, and the quantity of CAR T cells in CSF did not correlate with the neurotoxicity severity ($P = 0.404$; Fig. 4C).

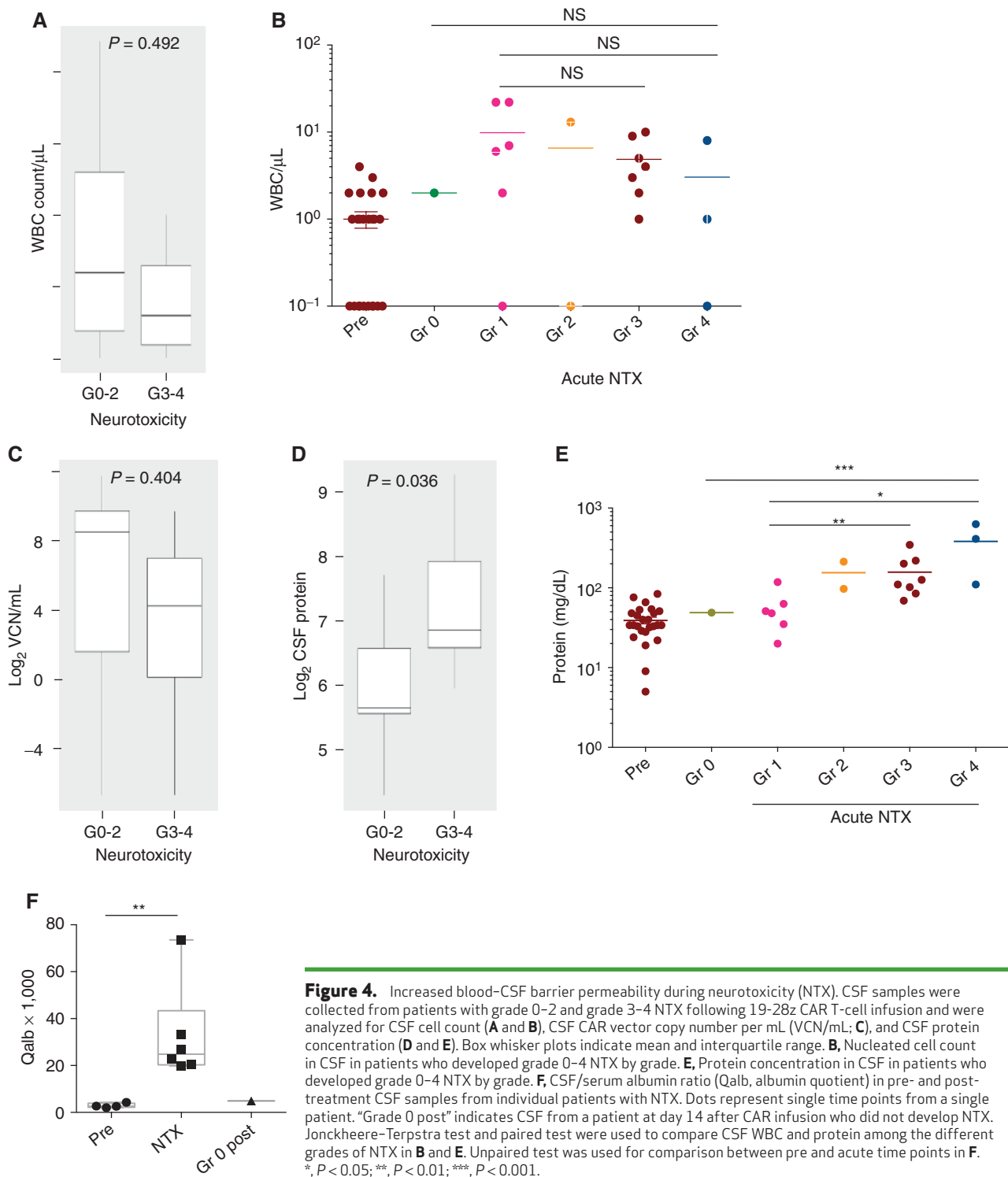
Notably, posttreatment CSF protein levels (Fig. 4D and E; $P = 0.036$) and CSF/serum albumin quotients (Qalb; Fig. 4F) were significantly elevated in patients with neurotoxicity compared to pretreatment values, and CSF protein concentration correlated with the grade of neurotoxicity (Fig. 4E). Elevated CSF protein and Qalb indicate blood–CSF barrier dysfunction or a decreased CSF flow rate correlating with neurotoxicity (21). There was no correlation between the CSF cell count and CSF protein concentration. These findings indicate that there is increased blood–CSF barrier permeability during neurotoxicity that may occur by a distinct mechanism from CAR T or other cell accumulation in CSF.

Serum cytokines can potentially have greater access to the CNS during situations of increased blood–CSF barrier permeability. We found several cytokines to be significantly elevated in the CSF of patients with severe neurotoxicity, including IL1a, IL6, IL10, G-CSF, TNF α , IFN γ , IFN $\alpha 2$, FLT3L, eotaxin, fractalkine, and GRO (Fig. 5A). Notably, in the comparison of matched serum and CSF cytokines in 7 patients with severe neurotoxicity and 4 with mild neurotoxicity, IL8, IP10, and MCP1 were markedly elevated in the CSF of severely affected patients relative to blood (Fig. 5B), suggesting local CNS production of these cytokines. IL6 was also elevated in CSF relative to blood, although not reaching statistical significance. We found no correlation between the CSF cell count and any of the CSF-enriched cytokines ($P = 0.83$). In contrast, blood–CSF barrier disruption was significantly correlated with CSF levels of IL8, IL10, IFN γ , G-CSF, FLT3L, and GRO (Supplementary Table S3).

The clinical and radiographic characteristics suggestive of excitotoxicity after CD19 CAR T cells led us to hypothesize that endogenous excitatory agonists such as glutamate (Glut) and quinolinic acid (QA) are perturbed during neurotoxicity. Glut is the predominant excitatory neurotransmitter in the adult mammalian brain and, through its interactions with NMDA and α -amino-3-hydroxy-5-methyl-4-isoxazolepropionic acid (AMPA) receptors, is implicated in seizures and certain CNS disorders, and QA is an endogenous agonist of the NMDA receptor produced locally in the brain by microglia and macrophages. We analyzed the levels of these metabolites in the CSF of 13 patients for whom CSF samples were available prior to treatment and/or during the onset of neurologic symptoms. In this cohort, we observed significantly elevated levels of both QA and Glut in CSF during neurotoxicity compared to pretreatment, and found low levels of QA and Glut at day 14 after infusion in a patient who did not develop neurotoxicity (Fig. 5C). Together, these data suggest a link between elevated levels of CSF cytokines during neurotoxicity and increased concentrations of excitatory agonists QA and Glut in the CSF.

DISCUSSION

Clinical trials of CD19 CAR T therapy have consistently reported a significant incidence of neurotoxicity regardless of the CAR constructs, patient population, or disease subtype. In our series of 53 adult patients with relapsed B-ALL treated with 19-28z CAR T cells, we observed mild (grades 1–2) neurotoxicity in 11 patients (20.8%) and severe (grades 3–4) neurotoxicity in 22 patients (41.5%). No patient developed grade 5 neurotoxicity and no diffuse cerebral edema



was observed in this trial. The rate of neurotoxicity observed in our study is comparable with other studies of CD19 CAR T cells incorporating either CD28 or 4-1BB costimulation (3, 4, 6). Therefore, CD19 CAR T-cell design does not appear to affect the occurrence of neurotoxicity, although there has been no direct head-to-head comparison of costimulatory molecule effect on risk.

We confirmed previously reported findings that neurotoxicity is significantly correlated with *in vivo* CAR T-cell expansion and high pretreatment disease burden, two factors that reflect the association with increased *in vivo* CAR T-cell numbers. Although other studies have additionally shown an association between severe neurotoxicity and higher infused cell dose (5, 22), we did not observe such an association. This

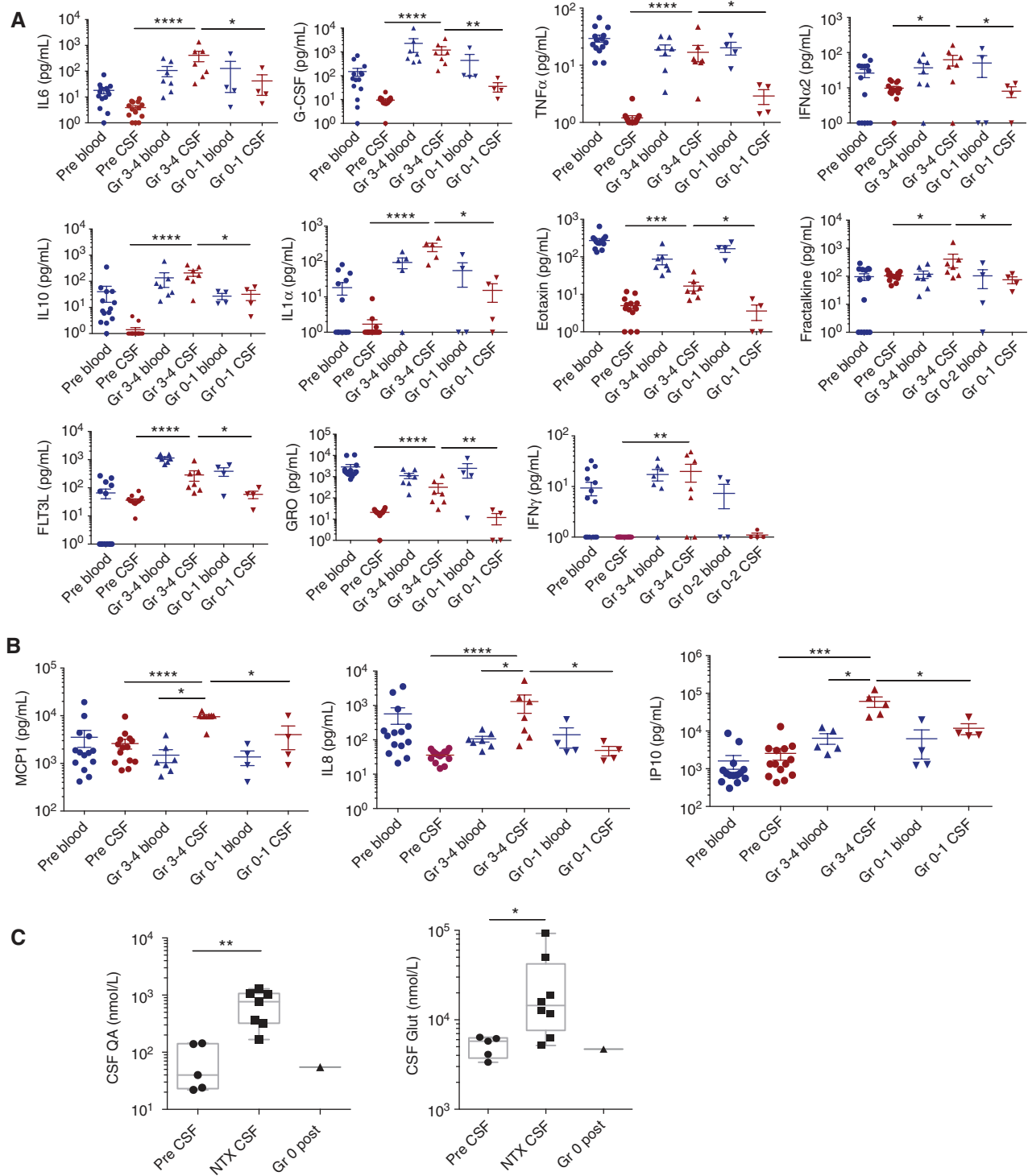


Figure 5. Elevated cytokine concentrations and excitatory neurotoxins in CSF during neurotoxicity (NTX). CSF was collected from patients with or without severe NTX. **A** and **B**, Concentrations of cytokines in paired serum and CSF samples obtained from patients who developed grade 0–1 ($n = 4$) or grade 3–4 ($n = 7$) NTX. There was no CSF from patients with grade 2 available for cytokine analysis. **A**, CSF cytokines with significantly higher levels in severe NTX (grade 3–4) than mild (grade 0–1) NTX. **B**, Cytokines with significantly higher levels in CSF than blood during severe NTX. **C**, NMDA receptor agonists quinolinic acid (QA) and glutamate (GLUT) in pretreatment CSF and CSF collected from individual patients during NTX. Dots represent time points from a single patient. “Grade 0 post” indicates CSF from a patient at day 14 after CAR infusion who did not develop NTX. P values in **A** and **B** were calculated using Wilcoxon test (two-sided). Unpaired test was used for comparison between pre and NTX time points in **C**. *, $P < 0.05$; **, $P < 0.01$; ***, $P < 0.001$; ****, $P < 0.0001$.

Downloaded from <http://aacrjournals.aacrjournals.org/cancerdiscovery/article-pdf/18/8/958/1840894/958.pdf> by guest on 27 August 2022

is possibly because patients in our trial received a low or high CAR T-cell dose (1×10^6 vs. 3×10^6 CAR T cells/kg) based on disease burden, with patients with higher disease burden receiving the lower dose of cells. An analysis of the cerebral edema-related deaths in the phase II ROCKET study, which used a similar CAR product to our phase I trial, demonstrated that early and rapid CAR T-cell expansion and a rise in IL15 levels are the primary contributors to cerebral edema (14). Moreover, it has been shown in the ROCKET study and by others (7) that the early and rapid expansion of CAR T cells is correlated with higher levels of IL15, which can be increased by the use of fludarabine and cyclophosphamide conditioning. Although we did not observe any cerebral edema or grade 5 neurotoxicity on our trial, we found day 3 and peak levels of IL15 correlated with development of severe neurotoxicity. By day 3 after infusion, those patients with high IL15, low EGF, and high IL10 have high risk of developing severe neurotoxicity (10/10; 100%; 95% CI, 69–100). Interestingly, IL15 appears to play a role in neurotoxicity and CRS in patients receiving lymphodepleting chemotherapy followed by haplo-NK adoptive transfer plus subcutaneous rIL15 (23). This adds to the growing list of immunotherapies, including the bispecific anti-CD3/CD19 T-cell engager blinatumomab, anti-CD22 CAR, and recently anti-CD20 CAR in a nonhuman primate model, that have a similar neurotoxicity profile. In light of this, it seems less likely that neurotoxicity results from direct targeting of CD19 antigen either on occult brain resident tumor cells or on nontumor elements in the CNS.

We found neurotoxicity to be significantly associated with early systemic inflammation and CRS, confirming findings from multiple prior studies with different CAR constructs. This association along with a potential role of IL6 in endothelial cell damage (24, 25) suggests that mitigation or prevention of severe CRS may lead to a lower incidence of severe neurotoxicity. Several groups have examined an early intervention strategy with tocilizumab, which decreased the rate of severe CRS, but did not affect the frequency of severe neurotoxicity (15, 26). Similarly, we observed that tocilizumab therapy alone did not ameliorate neurologic symptoms, whereas it readily improved CRS. Suboptimal response of neurotoxicity to tocilizumab may be due to elevation of multiple cytokines in addition to IL6 in patients with severe neurotoxicity, or because tocilizumab induces a transient increase of serum IL6 which might increase CNS levels (27). Although we observed a transient increase of serum IL6 after tocilizumab administration (Supplementary Fig. S2), 7 of 16 patients (43.7%) developed their most severe symptoms either prior to or on the day of tocilizumab administration, and the association between tocilizumab and worsening of neurotoxicity remains unclear.

An association between angiopoietin levels and CAR-associated neurotoxicity has recently been reported with a 4-1BB-containing CAR construct (11). We sought to determine whether these findings were generalizable to our large patient cohort treated with a CAR construct incorporating a different costimulatory domain CD28. Similar to the previous finding, we found a significant correlation between severe neurotoxicity and higher ANG2:ANG1 ratios. However, in our cohort, a dysregulated ANG–TIE2 axis was driven by lower levels of ANG1 and not higher levels of ANG2, whereas elevated ANG2 levels were associated with severe CRS. This

finding suggests that although endothelial activation associated with elevated ANG2 and CRS may prime for neurotoxicity, it is not sufficient and additional factors are required for neurotoxicity to fully develop. Further, because platelets are the primary cellular source of ANG1 (28), an association between low baseline platelet counts and neurotoxicity may be explained by low ANG1 levels and suggests that platelets may be a modifiable risk factor for endothelial activation.

Our data also underscore the critical role that endothelial damage and blood–CSF barrier dysfunction play in CAR-associated neurotoxicity. We observed elevated CSF protein and Qalb, indicating blood–CSF barrier dysfunction (21), correlated with neurotoxicity. Additional support for the link between CAR-associated neurotoxicity and endothelial cell damage comes from posterior reversible encephalopathy syndrome (PRES) and acute necrotizing encephalopathy (ANE), clinical neurologic syndromes characterized by similarities of clinical presentation and pathology with endothelial cell damage and systemic inflammation (29, 30). PRES often occurs in the setting of hypertension, when there is a breakdown of cerebral autoregulation, but may also be induced by inflammation conditions in the absence of hypertension (29). ANE is an exaggerated immune response that occurs after influenza and other viral infections; affected individuals develop vascular leakiness, DIC, high levels of serum cytokines, convulsions, and behavior abnormalities, culminating in coma (30). Four patients imaged during acute neurotoxicity in our study had a pattern of T2/FLAIR hyperintensities in the bilateral thalami and brainstem with a striking resemblance to both ANE and central-variant PRES (31). Other studies of CD19 CAR T cells with fatal cerebral edema cases (11, 14) reported the brain pathophysiology reminiscent of ANE brain autopsy specimens with venous and capillary congestion with hemorrhage within the thalamus and numerous CD68-positive macrophages (32, 33). The similarities between PRES, ANE, and CAR neurotoxicity suggests a common pathophysiology involving endothelium and the existence of a continuum between high-grade neurotoxicity and catastrophic cerebral edema cases.

Recently, a nonhuman primate model of CAR neurotoxicity found CAR and non-CAR T-cell infiltration into the CSF and brain parenchyma consistent with encephalitis (16). What is unclear is if these T cells are bystanders or active players in the development and maintenance of neurotoxicity symptoms. We observed that T-cell and WBC infiltration in the CSF does not correlate with the severity of neurotoxicity. In addition, we and others have observed that CAR T cells accumulate in the CSF after neurotoxicity resolves, and that CAR T cells can be found in the CSF of patients without neurotoxicity (10). Therefore, the role of T-cell infiltration into the CNS is unclear. It is possible that CSF profiling does not reflect the degree of parenchymal CNS infiltration which may be causing pathology. However, our data suggest that CAR infiltration into the CSF *per se* is not responsible for severe neurologic symptoms, and this finding is also consistent with the absence of neurotoxicity in 1 patient after receiving intrathecal and intratumoral administration of CAR T cells for recurrent glioblastoma (34).

Our finding of elevated levels of the NMDA receptor agonists QA and Glut in the CSF during neurotoxicity suggests a

mechanism by which CSF cytokines, such as those we found elevated during severe neurotoxicity (i.e., MCP1, IL6, IL8, IP10, IFN α 2, IFN γ , and TNF α), may trigger neurotoxicity independently of T cells. MCP1) is a chemokine produced by macrophages, microglia, activated astrocytes, and endothelial cells that is an activator of macrophage function and plays a crucial role in recruiting monocytes and macrophages to the brain (35, 36). Elevated concentrations of MCP1, IP10, IL6, and IL8 may be indicative of activated microglia, macrophages, or astrocytes responding to systemic inflammation and endothelial damage (37, 38). Activated microglia or infiltrating bloodstream monocytes and macrophages can produce and secrete large amounts of QA during CNS inflammation when stimulated by IFN α 2 and IFN γ (39, 40). Through its endogenous agonist activity at the NMDA receptor, QA is known to participate in seizures (41) and a variety of human neurologic and psychiatric disorders (42). QA induces a marked expression of TNF α , IL6, and MCP1 by astrocytes (43, 44), stimulates Glut production and inhibits its reuptake by astrocytes (45), and alters the integrity and cohesion of the blood-brain barrier (46), potentially providing a feed-forward mechanism for continued dysfunction. Mutation of the amino- β -carboxymuconate-semialdehyde-decarboxylase (ACMSD) gene results in elevated levels of QA, and affected individuals develop myoclonic tremor, epilepsy, and parkinsonism (47), further linking this metabolite to the unique constellation of neurotoxicity symptoms. In addition, elevated CSF TNF α may potentiate neurotoxicity by both increasing the production of cerebral Glut by cell types such as microglia and decreasing its clearance, resulting in increased concentration and availability to mediate excitotoxicity through NMDA and AMPA receptors (48). Together, our data suggest a novel mechanism for the symptoms observed during neurotoxicity following CD19 CAR therapy.

CD19-directed CAR and T cell-engaging therapies have demonstrated high antitumor efficacy across all hematologic malignancies but are associated with unique toxicities of CRS and neurotoxicity. Previous studies of clinical and biological factors associated with CRS have significantly improved the safety of the therapy and provided better management guidelines for CRS. There is yet no consensus with respect to which therapeutic interventions are most effective for preventing or reducing the severity or duration of neurologic symptoms. Our data suggest that interventions to reduce early inflammation, blood-CSF barrier disruption, myeloid cell accumulation or activation, QA and Glut quantity, or NMDA and AMPA receptor activity may further improve the safety of CD19 CAR T cells in B-ALL. Future work to understand the interplay between systemically and centrally produced cytokines and excitotoxic metabolites in the development of neurotoxicity will be invaluable to the design of studies to ensure safe delivery of CAR therapy.

METHODS

Trial Design and Oversight

We conducted a phase I clinical study of 19-28z CAR T cells in adult patients with CD19⁺ B-ALL at MSKCC (NCT01044069). All enrolled patients had relapsed or refractory disease in response to their previous treatment. The primary objective of the study was to

assess the safety of 19-28z CAR T cells, and the secondary objective was to assess the efficacy. The protocol was approved by the human studies review boards and granted FDA breakthrough status in 2014. All patients provided the written informed consent to participate in the study, and all clinical investigation was conducted according to the Declaration of Helsinki principles. The study included 3 stages, designed to evaluate the safety and efficacy of two different doses of CAR T cells (1×10^6 vs. 3×10^6 CAR T cells/kg) and conditioning chemotherapy regimens (fludarabine + cyclophosphamide vs. cyclophosphamide). After leukapheresis, patients received interim therapy at the treating physician's discretion. All patients underwent bone marrow evaluations after interim therapy and immediately before T-cell infusion.

Toxicity Assessment

CRS was graded according to the MSKCC CRS grading system (Supplementary Table S4). Severe CRS was defined as \geq grade 3. Neurotoxicity was prospectively graded according to National Cancer Institute common terminology criteria for adverse events (CTCAE) v4.03 by the principal investigator (J.H. Park). An independent retrospective review of the electronic medical record was performed by a neurologist (B.D. Santomaso) who assigned daily neurotoxicity grades to the AE terms according to CTCAE v4.03. Discrepancies were adjudicated by consensus review. All patients developing neurologic symptoms were evaluated by the neurology consult service and followed with daily neurologic assessments until neurologic symptom resolution. Severe neurotoxicity was defined as \geq grade 3 toxicity with the exception that any seizure (including grade 1 or 2 by CTCAE criteria) was included as severe neurotoxicity.

Cytokine Analysis

Cytokine profiles were analyzed from blood and CSF samples using the Luminex FlexMAP 3-D system and commercially available 38-plex cytokine detection assays as previously described (1, 49). Serum ANG1, ANG2, and CSF and serum albumin concentrations were evaluated using the Meso Scale Diagnostics platform and read on an MSD QuickPlex SQ 120 imager. Data were analyzed using the MSD Discovery Workbench software. A 4-parameter logistic fit calibration curve was generated for each analyte using the standards to calculate the concentration of each sample.

Lumbar Punctures and CSF Samples

CSF was collected from patients before conditioning chemotherapy (baseline) and during acute neurotoxicity, whenever feasible. CSF samples were analyzed for cell counts, glucose, protein, and cytology. In addition, CSF samples were evaluated for the presence of CAR T cells by PCR (1) and for cytokines as previously described (49).

LC/MS Measurement of Glutamate and Quinolinic Acid in CSF

LC/MS grade solvents were purchased from Fisher Scientific; QA, Glut, and $^{13}\text{C}_5,^{15}\text{N}$ -Glut [internal standard (ISTD)] were purchased from Sigma, and D3-QA acid (ISTD) was purchased from Buchem BV. Human CSF was thawed on ice, and 100 μL was extracted with 400 μL methanol containing ISTDs (0.4 $\mu\text{mol/L}$ D3-QA, 2.5 $\mu\text{mol/L}$ $^{13}\text{C}_5,^{15}\text{N}$ -Glut). Samples were vortexed, incubated at -20°C for 30 minutes to precipitate protein, centrifuged at $20,000 \times g$ for 15 minutes at 4°C , and the supernatant dried in a Genevac evaporator (SP Scientific). Samples were resuspended in 100 μL 0.4 % formic acid in water prior to HPLC/MS-MS analysis using a Thermo Vantage triple-quadrupole tandem mass spectrometer operating in positive ionization mode. Chromatographic separation was performed using an Agilent 1260 infinity binary pump, Acquity

UPLC HSS T3 column (2.1 × 100 mm, 1.8 μm, Waters), and MayLab column oven held at 35°C. Data were acquired and processed using TraceFinder 4.1 software (Thermo). Calibration curves were from 2.5 nmol/L to 10 μmol/L for QA and 10 nmol/L to 20 μmol/L for Glut. QC samples were prepared by standard addition in human spinal fluid (Golden West Biologicals) at 20 nmol/L, 200 nmol/L, and 2 μmol/L for QA or 40 nmol/L, 400 nmol/L, and 4 μmol/L for Glut and confirmed to be within ±20% accuracy.

19-28z CAR T-cell Expansion Assessment

Peripheral blood leukocytes were obtained from enrolled patients by leukapheresis, and CAR T cells were produced as previously described (1, 49). Persistence of 19-28z CAR T cells in patient peripheral blood was assessed by qPCR to determine vector copy number as previously described (1).

Statistical Analysis

Logistic regression was the primary method of analysis for evaluating associations between severe neurotoxicity and clinical and treatment variables, lab parameters, and cytokine levels as well as presence and grade of CRS. Predictors with a highly skewed distribution were log₂ transformed. In the instance of quasi-separation, Firth's adjustment to the likelihood was used to estimate odds ratios and obtain *P* values. Predictive models for severe neurotoxicity were developed using recursive partitioning, and accuracy of the resulting risk classifications were estimated using the leave-one-out method.

Disclosure of Potential Conflicts of Interest

B.D. Santomasso is a consultant/advisory board member for Juno Therapeutics, Kite/Gilead, and Novartis. J.H. Park is a consultant/advisory board member for Novartis, Juno Therapeutics, and Kite Pharma. L.M. DeAngelis is on the scientific advisory board of Juno Therapeutics. R.J. Brentjens reports receiving a commercial research grant from Juno Therapeutics and has ownership interest (including stock, patents, etc.) in the same. No potential conflicts of interest were disclosed by the other authors.

Authors' Contributions

Conception and design: B.D. Santomasso, J.H. Park, D. Salloum, I. Riviere, M. Gonen, H.-G. Wendel, M. Sadelain, R.J. Brentjens

Development of methodology: B.D. Santomasso, J.H. Park, D. Salloum, J.R. Cross, H. Liu, R.J. Brentjens

Acquisition of data (provided animals, acquired and managed patients, provided facilities, etc.): B.D. Santomasso, J.H. Park, I. Riviere, E. Mead, E. Halton, T. Purdon, J.R. Cross, H. Liu, L.M. DeAngelis

Analysis and interpretation of data (e.g., statistical analysis, biostatistics, computational analysis): B.D. Santomasso, J.H. Park, I. Riviere, J. Flynn, X. Chen, D. Li, M. Gonen

Writing, review, and/or revision of the manuscript: B.D. Santomasso, J.H. Park, D. Salloum, I. Riviere, J. Flynn, J.R. Cross, B. Vachha, L.M. DeAngelis, D. Li, M. Gonen, H.-G. Wendel, R.J. Brentjens

Administrative, technical, or material support (i.e., reporting or organizing data, constructing databases): B.D. Santomasso, J.H. Park, X. Wang, B. Senechal, T. Purdon, Y. Bernal

Study supervision: J.H. Park, L.M. DeAngelis, Y. Bernal, H.-G. Wendel, M. Sadelain

Acknowledgments

We thank the patients who participated in this trial and their families, and the Cell Therapy and Cell Engineering Facility and the Cellular Therapeutics Center staffs for help with clinical trial management. This work was supported by NIH grants (5P01 CA0237669-38, 5P01 CA190174-02, and 1P50 CA192937-01A1), the Carson Family

Charitable Trust, the Emerald Foundation, the Mr. and Mrs. Goodwyn Commonwealth Fund, the Annual Terry Fox Run for Cancer Research organized by the Canada Club of New York, Kate's Team, the William Laurence and Blanche Hughes Foundation, the Experimental Therapeutics Center of Memorial Sloan Kettering Cancer Center, Juno Therapeutics, the Lake Road Foundation, the Memorial Sloan Kettering Cancer Center Support Grant (P30 CA008748), and the Parker Institute for Cancer Immunotherapy Pilot Grant. J.H. Park is supported by grants from the American Society of Clinical Oncology, the American Society of Hematology, the Leukemia and Lymphoma Society, and the National Comprehensive Cancer Center.

Received November 27, 2017; revised May 1, 2018; accepted June 6, 2018; published first June 7, 2018.

REFERENCES

- Brentjens RJ, Davila ML, Riviere I, Park J, Wang X, Cowell LG, et al. CD19-targeted T cells rapidly induce molecular remissions in adults with chemotherapy-refractory acute lymphoblastic leukemia. *Sci Transl Med* 2013;5:177ra38.
- Park JH, Geyer MB, Brentjens RJ. CD19-targeted CAR T-cell therapeutics for hematologic malignancies: interpreting clinical outcomes to date. *Blood* 2016;127:3312–20.
- Maude SL, Frey N, Shaw PA, Aplenc R, Barrett DM, Bunin NJ, et al. Chimeric antigen receptor T cells for sustained remissions in leukemia. *N Engl J Med* 2014;371:1507–17.
- Turtle CJ, Hanafi LA, Berger C, Gooley TA, Cherian S, Hudecek M, et al. CD19 CAR-T cells of defined CD4⁺:CD8⁺ composition in adult B cell ALL patients. *J Clin Invest* 2016;126:2123–38.
- Lee DW, Kochenderfer JN, Stetler-Stevenson M, Cui YK, Delbrook C, Feldman SA, et al. T cells expressing CD19 chimeric antigen receptors for acute lymphoblastic leukaemia in children and young adults: a phase 1 dose-escalation trial. *Lancet* 2015;385:517–28.
- Gardner RA, Finney O, Annesley C, Brakke H, Summers C, Leger K, et al. Intent-to-treat leukemia remission by CD19 CAR T cells of defined formulation and dose in children and young adults. *Blood* 2017;129:3322–31.
- Kochenderfer JN, Somerville RPT, Lu T, Shi V, Bot A, Rossi J, et al. Lymphoma remissions caused by anti-CD19 chimeric antigen receptor T cells are associated with high serum interleukin-15 levels. *J Clin Oncol* 2017;35:1803–13.
- Park JH, Riviere I, Gonen M, Wang X, Senechal B, Curran KJ, et al. Long-term follow-up of CD19 CAR therapy in acute lymphoblastic leukemia. *N Engl J Med* 2018;378:449–59.
- Neelapu SS, Locke FL, Bartlett NL, Lekakis LJ, Miklos DB, Jacobson CA, et al. Axicabtagene ciloleucel CAR T-cell therapy in refractory large B-cell lymphoma. *N Engl J Med* 2017;377:2531–44.
- Mueller KT, Maude SL, Porter DL, Frey N, Wood P, Han X, et al. Cellular kinetics of CTL019 in relapsed/refractory B-cell acute lymphoblastic leukemia and chronic lymphocytic leukemia. *Blood* 2017;130:2317–25.
- Gust J, Hay KA, Hanafi LA, Li D, Myerson D, Gonzalez-Cuyar LF, et al. Endothelial activation and blood-brain barrier disruption in neurotoxicity after adoptive immunotherapy with CD19 CAR-T cells. *Cancer Discov* 2017.
- Frey NV, Levine BL, Lacey SF, Grupp SA, Maude SL, Schuster SJ, et al. Refractory cytokine release syndrome in recipients of chimeric antigen receptor (CAR) T cells. *Blood* 2014;124:2296.
- Brudno JN, Kochenderfer JN. Toxicities of chimeric antigen receptor T cells: recognition and management. *Blood* 2016;127:3321–30.
- Gilbert MJ. Severe neurotoxicity in the phase 2 trial of JCAR015 in adult B-ALL (ROCKET Study): analyses of patient, protocol and product attributes. Presented at 2017 SITC Annual Meeting, Session 102, 2017.
- Locke FL, Neelapu SS, Bartlett NL, Lekakis LJ, Jacobson CA, Braunschweig I, et al. Preliminary results of prophylactic tocilizumab after axicabtagene ciloleucel (axi-cel; KTE-C19) treatment for patients with

- refractory, aggressive non-Hodgkin lymphoma (NHL). *Blood* (ASH Abstract) 2017;130:1547.
16. Taraseviciute A, Tkachev V, Ponce R, Turtle CJ, Snyder JM, Liggitt HD, et al. Chimeric antigen receptor T cell-mediated neurotoxicity in non-human primates. *Cancer Discov* 2018;8:750–63.
 17. Neelapu SS, Tummala S, Kebriaei P, Wierda W, Gutierrez C, Locke FL, et al. Chimeric antigen receptor T-cell therapy – assessment and management of toxicities. *Nat Rev Clin Oncol* 2018;15:47–62.
 18. Ben-Ezra J, Sheibani K, Hwang DL, Lev-Ran A. Megakaryocyte synthesis is the source of epidermal growth factor in human platelets. *Am J Pathol* 1990;137:755–9.
 19. Hay KA, Hanafi LA, Li D, Gust J, Liles WC, Wurfel MM, et al. Kinetics and biomarkers of severe cytokine release syndrome after CD19 chimeric antigen receptor-modified T-cell therapy. *Blood* 2017;130:2295–306.
 20. Higgins SJ, Purcell LA, Silver KL, Tran V, Crowley V, Hawkes M, et al. Dysregulation of angiopoietin-1 plays a mechanistic role in the pathogenesis of cerebral malaria. *Sci Transl Med* 2016;8:358ra128.
 21. Reiber H. Flow rate of cerebrospinal fluid (CSF)—a concept common to normal blood-CSF barrier function and to dysfunction in neurological diseases. *J Neurol Sci* 1994;122:189–203.
 22. Fry TJ, Shah NN, Orentas RJ, Stetler-Stevenson M, Yuan CM, Ramakrishna S, et al. CD22-targeted CAR T cells induce remission in B-ALL that is naive or resistant to CD19-targeted CAR immunotherapy. *Nat Med* 2018;24:20–8.
 23. Cooley S, He F, Bachanova V, Vercellotti GM, DeFor TE, Curtisinger J, et al. Neurological consequences of cytokine release syndrome following subcutaneous recombinant IL-15 and haploidentical donor natural killer cell therapy for advanced acute myeloid leukemia. *Blood* (ASH Abstract) 2017;130:2649.
 24. Wassmann S, Stumpf M, Strehlow K, Schmid A, Schieffer B, Bohm M, et al. Interleukin-6 induces oxidative stress and endothelial dysfunction by overexpression of the angiotensin II type 1 receptor. *Circ Res* 2004;94:534–41.
 25. Esteve E, Castro A, Lopez-Bermejo A, Vendrell J, Ricart W, Fernandez-Real JM. Serum interleukin-6 correlates with endothelial dysfunction in healthy men independently of insulin sensitivity. *Diabetes Care* 2007;30:939–45.
 26. Gardner R, Leger KJ, Annesley CE, Summers C, Rivers J, Gust J, et al. Decreased rates of severe CRS seen with early intervention strategies for CD19 CAR-T cell toxicity management. *Blood* (ASH Abstract) 2016;128:586.
 27. Nishimoto N, Terao K, Mima T, Nakahara H, Takagi N, Kakehi T. Mechanisms and pathologic significances in increase in serum interleukin-6 (IL-6) and soluble IL-6 receptor after administration of an anti-IL-6 receptor antibody, tocilizumab, in patients with rheumatoid arthritis and Castleman disease. *Blood* 2008;112:3959–64.
 28. Brouwers J, Noviyanti R, Fijnheer R, de Groot PG, Trianty L, Mudaliana S, et al. Platelet activation determines angiopoietin-1 and VEGF levels in malaria: implications for their use as biomarkers. *PLoS One* 2014;8:e64850.
 29. Granata G, Greco A, Iannella G, Granata M, Manno A, Savastano E, et al. Posterior reversible encephalopathy syndrome—Insight into pathogenesis, clinical variants and treatment approaches. *Autoimmun Rev* 2015;14:830–6.
 30. Morishima T, Togashi T, Yokota S, Okuno Y, Miyazaki C, Tashiro M, et al. Encephalitis and encephalopathy associated with an influenza epidemic in Japan. *Clin Infect Dis* 2002;35:512–7.
 31. McKinney AM, Jagadeesan BD, Truwit CL. Central-variant posterior reversible encephalopathy syndrome: brainstem or basal ganglia involvement lacking cortical or subcortical cerebral edema. *AJR Am J Roentgenol* 2013;201:631–8.
 32. Alvarenga RM, Neri VC, Mendonca T, Camargo S. Acute encephalopathy with bilateral thalamotegmental involvement and a benign course: a case report from Brazil. *BMJ Case Rep* 2011;2011.
 33. Ishii N, Mochizuki H, Moriguchi-Goto S, Shintaku M, Asada Y, Taniguchi A, et al. An autopsy case of elderly-onset acute necrotizing encephalopathy secondary to influenza. *J Neurol Sci* 2015;354:129–30.
 34. Brown CE, Alizadeh D, Starr R, Weng L, Wagner JR, Naranjo A, et al. Regression of glioblastoma after chimeric antigen receptor T-cell therapy. *N Engl J Med* 2016;375:2561–9.
 35. Fuentes ME, Durham SK, Swerdel MR, Lewin AC, Barton DS, Megill JR, et al. Controlled recruitment of monocytes and macrophages to specific organs through transgenic expression of monocyte chemoattractant protein-1. *J Immunol* 1995;155:5769–76.
 36. McManus CM, Weidenheim K, Woodman SE, Nunez J, Hesselgesser J, Nath A, et al. Chemokine and chemokine-receptor expression in human glial elements: induction by the HIV protein, Tat, and chemokine autoregulation. *Am J Pathol* 2000;156:1441–53.
 37. Ehrlich LC, Hu S, Sheng WS, Sutton RL, Rockswold GL, Peterson PK, et al. Cytokine regulation of human microglial cell IL-8 production. *J Immunol* 1998;160:1944–8.
 38. Zink MC, Coleman GD, Mankowski JL, Adams RJ, Tarwater PM, Fox K, et al. Increased macrophage chemoattractant protein-1 in cerebrospinal fluid precedes and predicts simian immunodeficiency virus encephalitis. *J Infect Dis* 2001;184:1015–21.
 39. Heyes MP, Saito K, Major EO, Milstien S, Markey SP, Vickers JH. A mechanism of quinolinic acid formation by brain in inflammatory neurological disease. Attenuation of synthesis from L-tryptophan by 6-chlorotryptophan and 4-chloro-3-hydroxyanthranilate. *Brain* 1993;116:1425–50.
 40. Pemberton LA, Kerr SJ, Smythe G, Brew BJ. Quinolinic acid production by macrophages stimulated with IFN-gamma, TNF-alpha, and IFN-alpha. *J Interferon Cytokine Res* 1997;17:589–95.
 41. Schwarcz R, Brush GS, Foster AC, French ED. Seizure activity and lesions after intrahippocampal quinolinic acid injection. *Exp Neurol* 1984;84:1–17.
 42. Lugo-Huitron R, Ugalde Muniz P, Pineda B, Pedraza-Chaverri J, Rios C, Perez-de la Cruz V. Quinolinic acid: an endogenous neurotoxin with multiple targets. *Oxid Med Cell Longev* 2013;2013:104024.
 43. Schieffer J, Topper R, Schmidt W, Block F, Heinrich PC, Noth J, et al. Expression of interleukin 6 in the rat striatum following stereotaxic injection of quinolinic acid. *J Neuroimmunol* 1998;89:168–76.
 44. Guillemin GJ, Croitoru-Lamoury J, Dormont D, Armati PJ, Brew BJ. Quinolinic acid upregulates chemokine production and chemokine receptor expression in astrocytes. *Glia* 2003;41:371–81.
 45. Tavares RG, Tasca CI, Santos CE, Alves LB, Porciuncula LO, Emanuelli T, et al. Quinolinic acid stimulates synaptosomal glutamate release and inhibits glutamate uptake into astrocytes. *Neurochem Int* 2002;40:621–7.
 46. St'astny F, Skultetyova I, Pliss L, Jezova D. Quinolinic acid enhances permeability of rat brain microvessels to plasma albumin. *Brain Res Bull* 2000;53:415–20.
 47. Marti-Masso JF, Bergareche A, Makarov V, Ruiz-Martinez J, Gorostidi A, Lopez de Munain A, et al. The ACMSD gene, involved in tryptophan metabolism, is mutated in a family with cortical myoclonus, epilepsy, and parkinsonism. *J Mol Med (Berl)* 2013;91:1399–406.
 48. Clark IA, Vissel B. Excess cerebral TNF causing glutamate excitotoxicity rationalizes treatment of neurodegenerative diseases and neurogenic pain by anti-TNF agents. *J Neuroinflammation* 2016;13:236.
 49. Brentjens RJ, Riviere I, Park JH, Davila ML, Wang X, Stefanski J, et al. Safety and persistence of adoptively transferred autologous CD19-targeted T cells in patients with relapsed or chemotherapy refractory B-cell leukemias. *Blood* 2011;118:4817–28.